Introduction

In this proposal, we expect to obtain theoretical electron density distribution of target compounds. The electron density will be analyzed by Bader's Atoms in Molecule: a Quantum Theory (QTAIM).[1-3] Our interests are mainly focused on characterizing any kinds of chemical bonds, especially ultra short metal-metal multiple bonds such as Cr-Cr quintuple bond. Will the electron density distributions and topological properties of such M-M bond be the same as normal covalent bonds?

The concept of chemical bond was initiated by G. N. Lewis in 1916,[4] who described that a chemical single bond is formed when a pair of electrons was shared by two atoms. According to this concept, double bond can be described when two pairs of electrons are shared by two atoms and triple bond is three pairs of electrons, and so on. Lewis's concept was pictured completely by LCAO-MO method by Coulson and Fischer in 1949 for H_2 molecule[5]. The idea of two-electron bond was highlighted by F. A. Cotton[6]. Nowadays, the widely used concept to describe a single covalent chemical bond between two atoms is based on molecular orbital theory, in which a chemical bond is that a bonding orbital formed between the bonded atomic orbitals occupied by two electrons.

The maximum bond multiplicity was known as three between main group atoms, such as C≡C, before $[Re_2(Cl)_8]^{2-}$ was published in 1964[7]. $[Re_2(Cl)_8]^{2-}$ was already well known to have maximum bond multiplicity of four, i.e. a quadruple bond, with surprisingly short Re-Re distance of 2.24 Å. The quadruple bond can be qualitatively described as $\sigma^2\pi^4\delta^2$ configuration, 4 pairs of electrons were shared between two Re atoms, one σ, two π and one δ bond. After that, extensive interests were drawn on metal-metal bond. Hundreds of dichromium complexes were published before 2005. The statistics on the M-M distance of the complexes which contain metal-metal bond are shown in Figure 1. The most frequently synthesized Cr-Cr bond distance is 2.8 Å. There are dozens of cases have been recorded with another two frequently synthesized bond distances of 1.9 and 2.3 Å. The work on metal-metal multiple bond was also highlighted by F. A. Cotton in 1998[8]. In those cases, there are more than hundred complexes expected to have fBO = 4 but the bond distance difference between the shortest and the longest one is as large as 0.7 Å. This might be due to bridge ligand[9-12] or axial ligand effects[13,14].

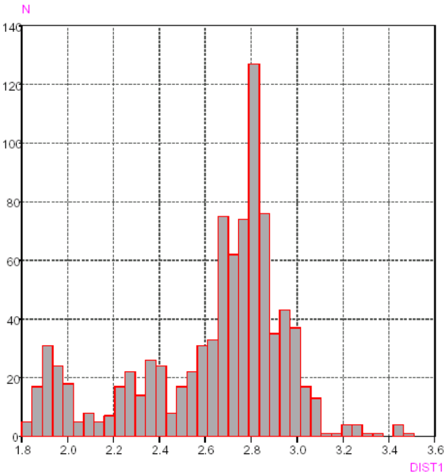

Figure 1 The statistics of Cr-Cr bonded complexes from crystal structure database with data base before 2008.

There are several cases with Cr-Cr distances in the range of 1.80 Å ~ 1.90 Å[15-22]. The Cr-Cr bonds of them were expected to be quadruply bonded. The first case is $Cr_2(DMP)_4$ (DMP = 2,6-dimethoxyphenyl) with Cr-Cr bond distance 1.847(1) Å[19]. Until 2005, one case claimed a five-fold bond with $\sigma^2\pi^4\delta^4$ 10 electronic configuration filling in five d-orbitals[23]. Accordingly, there are three possible candidates of 3d transition metal ion, Cr(I), Mn(II) and Fe(III), to form quintuple bond from overlapping of 5 d-orbitals.

In order to get the maximum bond multiplicity, Tailuan Nguyen et al. mentioned that low coordination number and low valence in metal are necessary for M-M multiple bonds[8]. The first fivefold bonding dichromium(I) complex, LCrCrL

(L= ArNC(H)NAr, Ar=C_6H_3-2,6(C_6H_3-2,6-*i*Pr_2)$_2$, where *i*Pr indicates isopropyl) was synthesized by Tailuan Nguyen et al. in 2005[23]. The valence of Cr atom in this complex is 1+ and coordination number is only two. The Cr-Cr bond length is 1.8351(4) Å with formal bond order (fBO) 5. The quintuple bond ($\sigma^2\pi^4\delta^4$) was formed from five d-orbitals of each metal atom.

Recently, Roos et al. found that a possible bond multiplicity of 6 may exist[24]. The shortest Cr-Cr bond distance of 1.66 Å in diatom molecules, Cr_2 indicates a formal bond order (fBO) of 6 but an effective bond order (eBO) of 3.5. Similarly, diatom molecules Mo_2 and W_2 with bond distance of 1.95 Å and 2.01 Å, respectively, have fBO of 6 but higher eBO of 5.2. The weaker M-M bond of Cr_2 is probably due to the more diffused electron distribution of 4s than 3d orbitals, which plays some role on the metal-metal repulsion. However, this difference in radial distributions decreases substantially in second- and third-row transition metal atoms. Later, the optimized geometries on the linear structure and trans-bent structure of PhCrCrPh molecules show that the linear one has shorter Cr-Cr bond distance, 1.678 Å, than trans-bent one, 1.752 Å[25]. Therefore, the Cr-Cr bond distance shorter than 1.8 Å is feasible and it is successfully synthesized recently. Two remarkably short metal-metal bond distance of dichromium(I) complexes, $Cr_2(I)L_2$, published by Noor[26] (L=[6-(2,4,6-tri-isopropyl phenyl)pyridin-2-yl](2,4,6-trimethylphenyl)amide) with Cr-Cr bond distances 1.749(2) Å, fBO=5.0 and by Tsai[27,28] (L = Ar^{xyl}NC(H)NAr^{xyl}, Ar^{xyl} = 2,6-Me_2-C_6H_3) with Cr-Cr = 1.8169(7) Å, fBO = 4.5 and Cr-Cr = 1.7397(9) Å, fBO = 5.0. In Tsai's group, some other quintuple bonded di-chromium complexes are also synthesized[27,28]. The complex $Cr_2(mhp)_4$[20] is expected that the ground state with Cr-Cr quadruple bond is the major component (55%) according to limited CI calculation[29].

It is extremely interesting to note that the experimental charge density analysis is still the best and the most direct way of characterizing the chemical bond, especially such short metal-metal bond. The Cr-Cr quadruple bond characters have been claimed by Benard in the point of view of experimental deformation density around 1980[29-31]. Large area of excess electron density off bond axis was observed which could be interpreted as the characters of π and δ bonds. At that time, the first experimental electron density study on $Mo_2(CH_3CO_2)_4$ with Mo-Mo distance of 2.0885(5) Å was performed[32]. After this, although amount of complexes with very short metal-metal bond were synthesized, the electron density studied on such complex was still rare. One Rh-Rh bonded complex was studied on theoretical Laplacian of charge density in 1990, however, the bond distance was long, 2.496 Å[33]. Until 1998, the charge density study on some metal complexes with unbridged metal-metal bond were published[34-36], charge density study on metal-metal bond launched into a new age again.

Introduction of Atoms in molecules: a Quantum Theory (QTAIM)

In experiments, X-ray diffraction is a unique and useful tool for mapping the charge density distribution in crystals[37]. Charge density analysis is realized by collecting very high resolution data from single crystal X-ray diffraction. This technique has been developed maturely by now. Solving structure has become a routine work by convenient software and powerful computer development. The total electron density is then modeled by Hansen and Coppens' multipole model published in 1978[38]. In theory, quantum calculation gives total electron density based on DFT calculation. QTAIM is a very useful tool to analyze the electron density distribution (like deformation electron density and Laplacian density), topological properties at bond critical points, Fermi-hole function and electrostatic potential. The inter-atomic interactions, like covalent bonding, ionic bonding, H-bond and van del Waal interaction can be classified according to the topological properties at bond critical point[39,40]. The process chart and related properties of charge density analyses are illustrated in Figure 2. More details of electron density study will be discussed later.

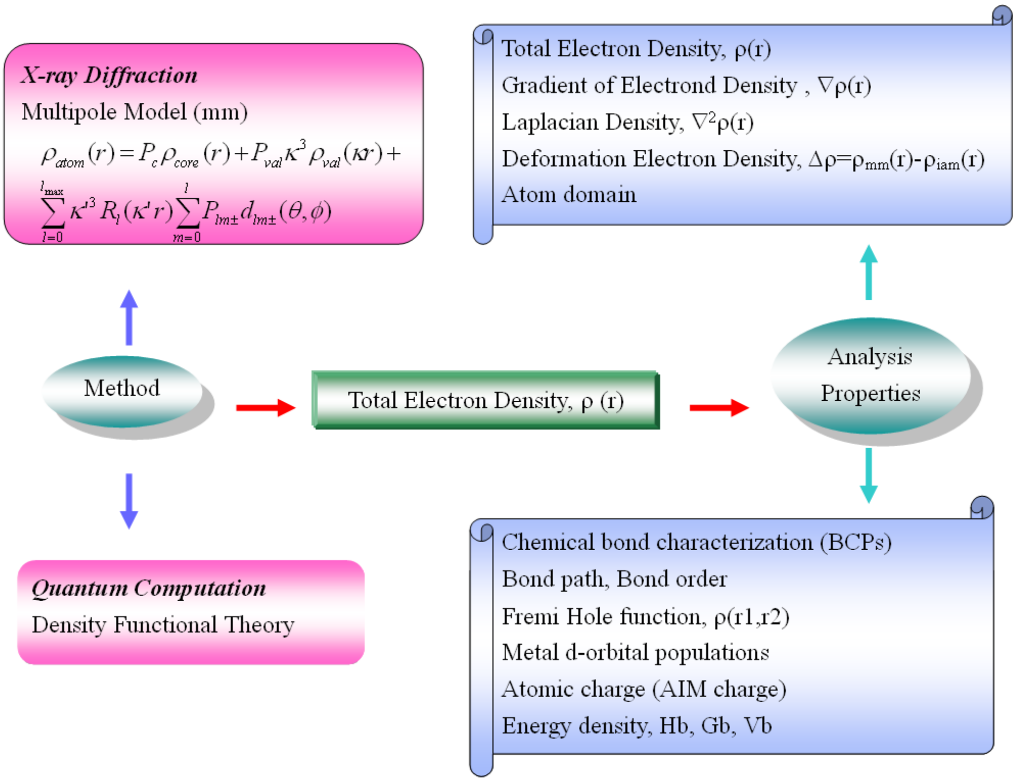

Figure 2 Procedures of electron density method.

All materials are composed of atoms. According to Bader’s theory, atom is an attractor in the scalar function. As atoms integrate into a molecule to form a rigid chemical bond, the electron density redistributes from spherical to aspherical shape in space, taking C_2H_4 as an example illustrated in Figure 3. The largest electron concentration (local maximum) is located at nucleus position. The electron density at midpoint of C-C bond is a local minimum along C-C bond direction and local maximum perpendicular to bond.

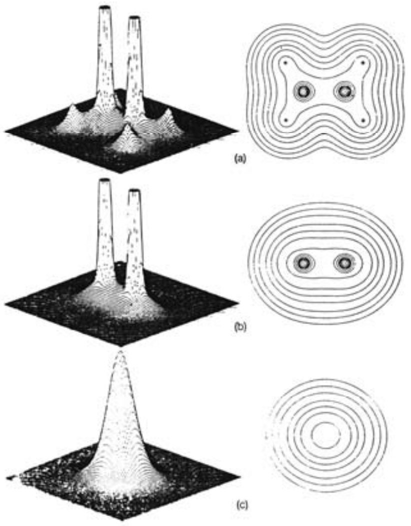

Figure 3 The total electron density of C_2H_4 molecule in 2D and 3D. (a) The molecule plane of C_2H_4. (b) The plane perpendicular to (a) contains only two carbon atoms. (c) The plane at the mid point of the C-C bond and perpendicular to (a) and (b)[1].

Secondary derivative of total electron density at any point (x,y,z) in space can be written as a Hessian matrix, *H*:

$$H(\rho)_{ij} = \begin{pmatrix} \frac{\partial^2\rho}{\partial x^2} & \frac{\partial^2\rho}{\partial x\partial y} & \frac{\partial^2\rho}{\partial x\partial z} \\ \frac{\partial^2\rho}{\partial y\partial x} & \frac{\partial^2\rho}{\partial y^2} & \frac{\partial^2\rho}{\partial y\partial z} \\ \frac{\partial^2\rho}{\partial z\partial x} & \frac{\partial^2\rho}{\partial z\partial y} & \frac{\partial^2\rho}{\partial z^2} \end{pmatrix} \cdots\cdots\cdots\cdots \text{eq (1)}$$

The critical points can be obtained as $\rho'(r) = 0$. Four types of critical points can be defined by rank and signature (denoted as (ω,σ)) where rank is the number of non-zero eigenvalues (as eq(8)) of the Hessian matrix at critical point and signature is the sum of the signs of the eigenvalues. Four kinds of critical points (CP) can be defined as nucleus (r_n), bond (r_b), ring (r_r) and cage (r_c) according to (ω,σ), as listed in Table 1. Three λ values (λ_1, λ_2, λ_3) are defined as second derivative of $\rho(r)$ at critical point along x, y and z directions, respectively. Therefore, the summation of diagonal terms of *H* can be defined as Laplacian, $\nabla 2\rho(r)$:

$$\nabla^2 \rho(r) = \frac{\partial^2}{\partial x^2}\rho(r) + \frac{\partial^2}{\partial y^2}\rho(r) + \frac{\partial^2}{\partial z^2}\rho(r) = \lambda_1 + \lambda_2 + \lambda_3 \qquad \text{............eq (2)}$$

A bond critical point is a saddle point on a surface, as shown in Figure 4. All trajectories end at BCP except the two trajectories alone bond direction, which start from BCP and end at nucleus critical points (r_n).

Table 1 The definitions and mathematical descriptions of four kinds of critical points[1].

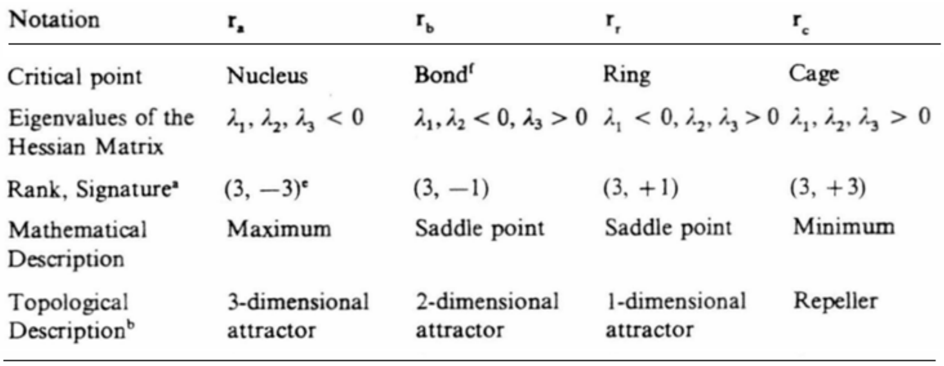

Notation	$\mathbf{r}_a$	$\mathbf{r}_b$	$\mathbf{r}_r$	$\mathbf{r}_c$
Critical point	Nucleus	Bond[f]	Ring	Cage
Eigenvalues of the Hessian Matrix	$\lambda_1, \lambda_2, \lambda_3 < 0$	$\lambda_1, \lambda_2 < 0, \lambda_3 > 0$	$\lambda_1 < 0, \lambda_2, \lambda_3 > 0$	$\lambda_1, \lambda_2, \lambda_3 > 0$
Rank, Signature[a]	(3, −3)[e]	(3, −1)	(3, +1)	(3, +3)
Mathematical Description	Maximum	Saddle point	Saddle point	Minimum
Topological Description[b]	3-dimensional attractor	2-dimensional attractor	1-dimensional attractor	Repeller

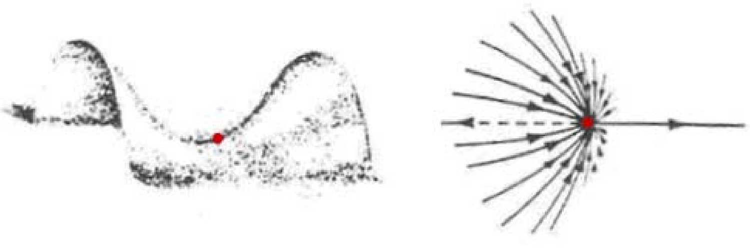

(3,-1)

Figure 4 Bond critical point (3,-1) (●) is a saddle point on a surface (left) and all trajectories (arrow curves) end at BCP except the two trajectories alone bond direction, which start from BCP and end at nucleus critical points (r_n)..

When electron redistributed around atoms, the boundary of an atom has to be defined. To define the boundary is very important for judging atomic charge and atomic basin. In Bader’s theory, the electron density between two bonded atoms is partitioned by zero-flux surface which is perpendicular to bond and pass through bond critical point (BCP). One side belongs to one atom and the other side belongs to other.

The boundary is defined by a zero-flux surface (ZFS) around the atom, $\nabla\rho(r)\cdot n(r) = 0$ where n(r) is the unit vector normal to the surface at r, $\nabla\rho(r)$ is first derivative of total electron density called gradient vector field, as the example of C_2H_4 shown in Figure 5. The spatial space surrounded by such ZFS is called an atom domain (or atomic basin, Ω). The atom domain of carbon atom in C_2H_4 is a triangular shape. The line of gradient vector field is named as trajectory.

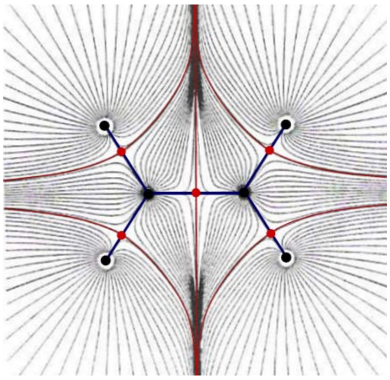

Figure 5 The gradient field, $\nabla\rho(r)$, of C_2H_4 molecule. The black dots (•) are nucleus bond critical points. The red dots (•) are bond critical points. The blue lines are bond path and the red lines/curves are zero-flux surfaces and The black curves are gradient vector field[1].

Atom in molecule is a quantum atom in QTAIM because the atom domain is surrounded by zero-flux surface which no trajectory crosses over. To define an atom in molecule is important and critical. This will seriously affect how the atomic charges are distributed between two atoms[41]. Therefore, Bader's AIM charge is defined as follows:

$$Q_A^{Bader} = Z_A - \int_{\Omega} \rho(r)dr \cdots\cdots\cdots\cdots \text{eq (3)}$$

where the first term Z_A is atomic number and the second term is number of electrons integrated all over the atomic basin of an atom.

Interaction between two atoms, no matter strong interaction like covalent bond or weak interaction like H-bond, can be identified by the topological properties associated with the bond critical point. The bond characterization between two atoms relies on whether the BCP and its accompanied bond paths are located. Bond path is the path starting from BCP along maximum charge density to the bonded nuclei, as the blue line shown in Figure 5. The bond paths and critical points can represent bonding structure. Some cases are shown in Figure 6. Linear bond path are observed in BH_3, CH_4, C_2H_6 and C_2H_2. The bonding structures of them are consistent with molecule structures. However, bending bond path are observed in C_3H_6, indicating the bond strain of such small ring structure. The bending bond path in B_2H_6 is due to three atoms sharing two electrons.

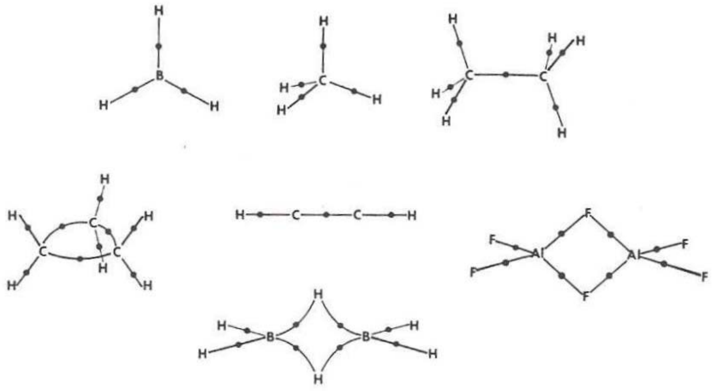

Figure 6 Some cases of bonding structures. Black dots represent bond critical points[1].

The topological properties at BCP, r_b, include electron density, $\rho(r_b)$, Laplacian, $\nabla^2\rho(r_b)$, bond ellipsoid, ε and energy densities ($H(r_b)$ for total energy density, $G(r_b)$ for kinetic energy density and $V(r_b)$ for potential energy density). Total energy density is the sum of kinetic energy density and potential energy density. The relationship of $G(r_b)$, $V(r_b)$ and $\nabla^2\rho(r_b)$ for a weakly bonded case is derived by Abramov and Espinosa[42,43]:

$$H(r_b) = G(r_b) + V(r_b) \cdots\cdots \text{eq 4}$$

$$2G(r_b) + V(r_b) = (1/4)\nabla^2 \rho(r_b) \cdots\cdots \text{eq 5}$$

According to the topological properties at BCPs, chemical bond can be simply classified into two types: shared interaction and closed-shell interaction based on the amplitude of $\rho(r_b)$ and the sign of $\nabla^2\rho(r_b)$. Shared interactions include covalent and polar covalent interactions. Closed-shell interactions include ionic and van der Waals (v.d.W.) bonds. The topological properties at bond critical points of some covalent bonded and ionic bonded compounds are listed in Table 2. For covalent case, it usually yields large ρ_b, large negative $\nabla^2\rho_b$, negative H_b and large G_b/ρ_b but G_b/ρ_b could be greater than 1 in polar covalent bonds, like C-O bond. On the contrary, small ρ_b, positive $\nabla^2\rho_b$, positive H_b and G_b/ρ_b > 1 can be classified as ionic cases.

Table 2 The topological properties at BCP of simple molecules with covalent (a) or ionic (b) bonds[1].

Bond A–B		Dist Å	ρ_b e/Å^3	$\nabla^2\rho_b$ e/Å^5	H_b H/Å^3	V_b H/Å^3	G_b H/Å^3	G_b/ρ_b H/e	H_b/ρ_b H/e	$\lvert V_b\rvert/G_b$
$H_3C–CH_3$	a	1.53	1.62	-13.64	-1.370	-1.790	0.420	0.26	-0.85	4.26
$H_2C{=}CH_2$	a	1.34	2.26	-23.83	-2.620	-3.570	0.950	0.42	-1.16	3.76
HC≡CH	a	1.21	2.66	-27.1	-3.790	-5.680	1.890	0.71	-1.42	3.01
$H_3C–OCH_3$	a	1.41	1.74	-9.94	-2.440	-4.190	1.750	1.01	-1.40	2.39
$H_2C{=}O$	a	1.21	2.76	-1.40	-4.630	-9.160	4.530	1.64	-1.68	2.02
C≡O	a	1.13	3.19	20.29	-5.620	-12.660	7.040	2.21	-1.76	1.80
Li–Cl	b	2.02	0.31	6.40	0.03	-0.38	0.41	1.33	0.11	0.92
Na–Cl	b	2.36	0.24	4.83	0.04	-0.26	0.30	1.24	0.15	0.88

However, many atom-atom interactions, such as metal-ligand and metal-metal bonds, are between share and close-shell interactions. These two type interactions are not enough to characterize all atom-atom interactions. In order to discuss more details of the interactions between share and close-shell interactions, some parameters were brought up by Bianchi[44], Macchi[36] and Espinosa[45]. Their classifications are listed in Table 3. According to the quantity of total energy density (H_b), kinetic energy density (K_b) and potential energy density (V_b) at BCP, Bianchi[44] classified close-shell interactions into dative, metallic, ionic and v.d.W. bonds based on the results of $Mn_2(CO)_{10}$. Macchi's study[36] on $Co_2(CO)_6(AsPh_3)_2$ showed five types of chemical interactions based on ρ_b, $\nabla^2\rho_b$, G_b/ρ_b and H_b/ρ_b as indicators. Espinosa's classification[45,46] is based on a comprehensive analysis of the topological and energetic properties of the electron density distribution involving from weak to strong interactions of F···H systems. The parameter used as boundary is defined according to eq 10 and eq 11. As $H_b=0$ gives $|V_b|/G_b=1$ and as $\nabla^2\rho_b=0$ gives $|V_b|/G_b=2$. H_b/ρ_b is defined as bond degree (BD) for the characterization of bond types. Espinosa interpreted this parameter as "the total pressure per electron density unit" or "the total energy per electron" at critical point[45]. It is indicated that the softening degree (SD) is defined when the value H_b/ρ_b is > 0, the weaker the interaction is; the greater the SD is. On the contrary, the covalence degree (CD) is defined when the value H_b/ρ_b is < 0, the stronger the interaction is; the greater the CD is. For instance, the value of BD on C−C bond becomes larger as the bond strength increases from ethane, ethylene to acetylene. This trend is also observed for C−O bond.

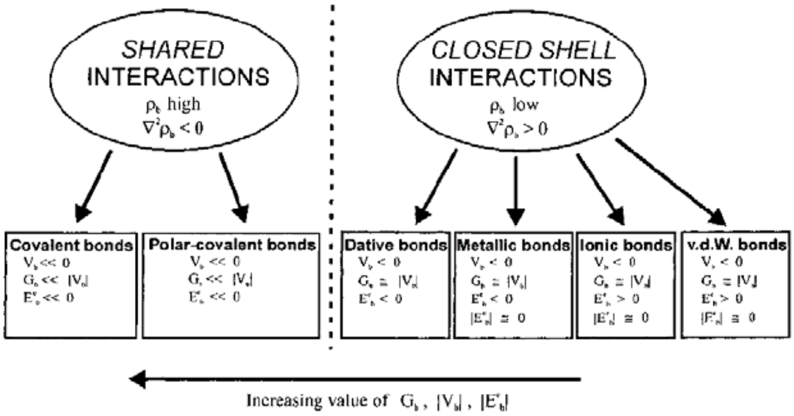

(a) Bianchi's classification[44] of $Mn_2(CO)_{10}$

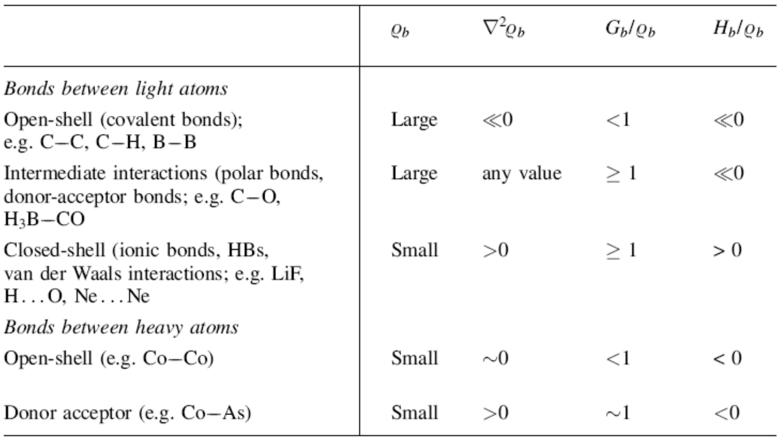

	ϱ_b	$\nabla^2\varrho_b$	G_b/ϱ_b	H_b/ϱ_b
Bonds between light atoms				
Open-shell (covalent bonds); e.g. C–C, C–H, B–B	Large	$\ll 0$	<1	$\ll 0$
Intermediate interactions (polar bonds, donor-acceptor bonds; e.g. C–O, H_3B–CO	Large	any value	≥ 1	$\ll 0$
Closed-shell (ionic bonds, HBs, van der Waals interactions; e.g. LiF, H. . . O, Ne. . . Ne	Small	>0	≥ 1	> 0
Bonds between heavy atoms				
Open-shell (e.g. Co–Co)	Small	~ 0	<1	< 0
Donor acceptor (e.g. Co–As)	Small	>0	~ 1	<0

(b) Macchi's classification of $Co_2(CO)_6(AsPh_3)_2$[36]

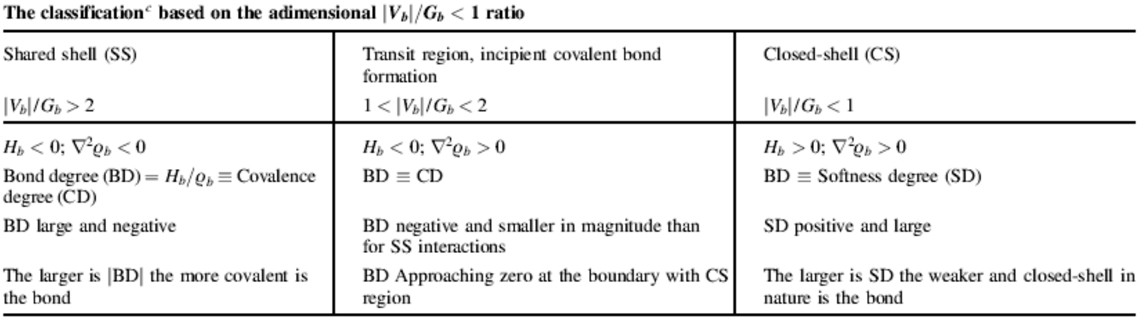

The classification[c] based on the adimensional $|V_b|/G_b < 1$ ratio

Shared shell (SS) $|V_b|/G_b > 2$	Transit region, incipient covalent bond formation $1 < |V_b|/G_b < 2$	Closed-shell (CS) $|V_b|/G_b < 1$
$H_b < 0$; $\nabla^2\varrho_b < 0$	$H_b < 0$; $\nabla^2\varrho_b > 0$	$H_b > 0$; $\nabla^2\varrho_b > 0$
Bond degree (BD) = $H_b/\varrho_b \equiv$ Covalence degree (CD)	BD $\equiv$ CD	BD $\equiv$ Softness degree (SD)
BD large and negative	BD negative and smaller in magnitude than for SS interactions	SD positive and large
The larger is |BD| the more covalent is the bond	BD Approaching zero at the boundary with CS region	The larger is SD the weaker and closed-shell in nature is the bond

(c) Espinosa's classification[45,46] of F···H systems

Table 3 Chemical bond classification by (a)Bianchi[44], (b)Macchi[36] and (c)Espinosa[45,46].

Reference

(1) Bader, R. F. W. *"Atoms in Molecules - a Quantum Theory", Oxford University Press* **1990**.

(2) Bader, R. F. W.; Macdougall, P. J.; Lau, C. D. H. *J Am Chem Soc* **1984**, *106*, 1594.

(3) Bader, R. F. W. *J Phys Chem A* **1998**, *102*, 7314.

(4) Lewis, G. N. *J. Am. Chem. Soc.* **1916**, *38*, 762.

(5) Coulson, C. A.; Fischer, I. *Philos Mag* **1949**, *40*, 386.

(6) Cotton, F. A.; Nocera, D. G. *Accounts Chem Res* **2000**, *33*, 483.

(7) Cotton, F. A.; Curtis, N. F.; Johnson, B. F. G.; Mague, J. T.; Wood, J. S.; Harris, C. B.; Robinson, W. R.; Lippard, S. J. *Science* **1964**, *145*, 1305.

(8) Cotton, F. A. *Inorg. Chem.* **1998**, *37*, 5710.

(9) Kok, R. A.; Hall, M. B. *J Am Chem Soc* **1983**, *105*, 676.

(10) Wiest, R.; Benard, M. *Chem Phys Lett* **1983**, *98*, 102.

(11) Kok, R. A.; Hall, M. B. *Inorg Chem* **1985**, *24*, 1542.

(12) Davy, R. D.; Hall, M. B. *J Am Chem Soc* **1989**, *111*, 1268.

(13) Cotton, F. A.; Extine, M. W.; Rice, G. W. *Inorg Chem* **1978**, *17*, 176.

(14) Berry, M.; Garner, C. D.; Hillier, I. H.; Clegg, W. *Inorg Chim a-Lett* **1980**, *45*, L209.

(15) Cotton, F. A.; Koch, S. *Inorg Chem* **1978**, *17*, 2021.

(16) Cotton, F. A.; Koch, S. A.; Millar, M. *Inorg Chem* **1978**, *17*, 2084.

(17) Cotton, F. A.; Koch, S. A.; Millar, M. *Inorg Chem* **1978**, *17*, 2087.

(18) Dionne, M.; Hao, S.; Gambarotta, S. *Can J Chem* **1995**, *73*, 1126.

(19) Cotton, F. A.; Koch, S.; Millar, M. *J Am Chem Soc* **1977**, *99*, 7372.

(20) Cotton, F. A.; Fanwick, P. E.; Niswander, R. H.; Sekutowski, J. C. *J. Am. Chem. Soc.* **1978**, *100*, 4725.

(21) Cotton, F. A.; Niswander, R. H.; Sekutowski, J. C. *Inorg Chem* **1978**, *17*, 3541.

(22) Cotton, F. A.; Millar, M. *Inorg Chem* **1978**, *17*, 2014.

(23) Nguyen, T.; Sutton, A. D.; Brynda, M.; Fettinger, J. C.; Long, G. J.; Power, P. P. *Science* **2005**, *310*, 844.

(24) Roos, B. O.; Borin, A. C.; Gagliardi, L. *Angew. Chem. Int. Ed.* **2007**, *46*, 1469.

(25) Brynda, M.; Gagliardi, L.; Widmark, P. O.; Power, P. P.; Roos, B. O. *Angewandte Chemie-International Edition* **2006**, *45*, 3804.

(26) Noor, A.; Wagner, F. R.; Kempe, R. *Angew. Chem. Int. Edit.* **2008**, *47*, 7246.

(27) Hsu, C. W.; Yu, J. S. K.; Yen, C. H.; Lee, G. H.; Wang, Y.; Tsai, Y. C. *Angew. Chem. Int. Ed.* **2008**, *47*, 9933.

(28) Tsai, Y. C.; Hsu, C. W.; Yu, J. S. K.; Lee, G. H.; Wang, Y.; Kuo, T. S. *Angew. Chem. Int. Ed.* **2008**, *47*, 7250.

(29) Mitschler, A.; Rees, B.; Wiest, R.; Benard, M. *J. Am. Chem. Soc.* **1982**, *104*, 7501.

(30) Benard, M. *J Am Chem Soc* **1978**, *100*, 7740.

(31) Benard, M.; Coppens, P.; Delucia, M. L.; Stevens, E. D. *Inorg Chem* **1980**, *19*, 1924.

(32) Hino, K.; Saito, Y.; Benard, M. *Acta Crystallogr., Sect. B* **1981**, *37*, 2164.

(33) Bo, C.; Poblet, J. M.; Benard, M. *Chem Phys Lett* **1990**, *169*, 89.

(34) Bianchi, R.; Gervasio, G.; Marabello, D., *Chem. Commun.,* **1998**, 1535.

(35) Jansen, G.; Schubart, M.; Findeis, B.; Gade, L. H.; Scowen, I. J.; McPartlin, M. *J Am Chem Soc* **1998**, *120*, 7239.

(36) Macchi, P.; Proserpio, D. M.; Sironi, A. *J Am Chem Soc* **1998**, *120*, 13429.

(37) Koritsanszky, T. S.; Coppens, P. *Chem Rev* **2001**, *101*, 1583.

(38) Hansen, N. K.; Coppens, P. *Acta Crystallogr A* **1978**, *34*, 909.

(39) Tsirelson, V. G.; Ozerov, R. P. *Taylor & Francis* **1996**.

(40) Coppens, P. *'X-Ray Charge Densities and Chemical Bonding' Oxford University Press; 1 edition* **1997**.

(41) Guerra, C. F.; Handgraaf, J. W.; Baerends, E. J.; Bickelhaupt, F. M. *J Comput Chem* **2004**, *25*, 189.

(42) Abramov, Y. A. *Acta Crystallogr A* **1997**, *53*, 264.

(43) Espinosa, E.; Molins, E.; Lecomte, C. *Chem Phys Lett* **1998**, *285*, 170.

(44) Bianchi, R.; Gervasio, G.; Marabello, D., *Inorg. Chem.,* **2000**, *39*, 2360.

(45) Espinosa, E.; Alkorta, I.; Elguero, J.; Molins, E., *J. Chem. Phys.,* **2002**, *117*, 5529.

(46) Gatti, C. *Z Kristallogr* **2005**, *220*, 399.